Journal of Computational Finance **21**(5), 97–129
DOI: 10.21314/JCF.2018.344

Research Paper

Pricing multivariate barrier reverse convertibles with factor-based subordinators

Marina Marena,[1] Andrea Romeo[1,2] and Patrizia Semeraro[3]

[1]Department of Economics and Statistics, University of Torino, Lungo Dora Siena, 100 A, 10153 Torino, Italy; email: marina.marena@unito.it

[2]Collegio Carlo Alberto, Piazza Arbarello 8, 10122 Torino, Italy; email: andrea.romeo@unito.it

[3]Department of Architecture and Design, Politecnico di Torino, Corso Duca degli Abruzzi, 24, 10129 Torino, Italy; email: patrizia.semeraro@polito.it

(Received December 9, 2015; revised June 17, 2016; accepted September 16, 2016)

ABSTRACT

In this paper, we study factor-based subordinated Lévy processes in their variance gamma (VG) and normal inverse Gaussian (NIG) specifications, and focus on their ability to price multivariate exotic derivatives. Both model specifications, calibrated to a data set of multivariate barrier reverse convertibles listed at the Swiss market, demonstrate good ability in capturing smile patterns and recovering empirical correlations. We show how the range of correlations spanned by each model is linked to the process marginal distributions. Our analysis finds that a trade-off exists between marginal and correlation fit. A sensitivity analysis is performed, showing how a product's characteristics and a model's features affect multibarrier reverse convertibles prices. Market and model prices are analyzed, and discrepancies are highlighted and explained.

Keywords: Lévy processes; multivariate subordinators; multivariate asset modeling; multivariate variance gamma (VG) process; multivariate normal inverse Gaussian (NIG) process; multibarrier reverse convertibles (MBRCs).

Corresponding author: P. Semeraro

Print ISSN 1460-1559 | Online ISSN 1755-2850

1 INTRODUCTION

Multi-asset derivative pricing is still an active field of research in financial modeling, calling for multivariate stochastic models that reproduce well-known stylized facts such as skewness and excess kurtosis of marginal return distributions. In this paper, we focus on a class of multivariate subordinated Lévy processes, namely, the $\rho\alpha$ models introduced by Luciano and Semeraro (2010). Among non-Gaussian multivariate processes, Lévy models are appealing in that they preserve analytical tractability.

An interesting testing ground for multivariate models is represented by the barrier reverse convertible on multiple assets, one of the most successful instruments on the Swiss market for structured financial products. The product consists specifically of a long position on a coupon bond and a short position on a worst-of down-and-in European put option. The worst-of feature requires a pricing model that can capture downside risk and the correlation between assets.

A study on a large data set of multibarrier reverse convertibles (MBRCs) has been conducted by Wallmeier and Diethelm (2012). They considered two multivariate Lévy processes with variance gamma (VG) marginal specifications: the model introduced by Leoni and Schoutens (2008) and the αVG model created by Semeraro (2008). Both models were shown to be able to capture option smile patterns, but they exhibit limitations in their ability to match empirically observed correlations. The $\rho\alpha$ models extend the αVG model by considering different marginal specifications and improving the correlation flexibility. In particular, two marginal specifications are considered in this work: VG and normal inverse Gaussian (NIG), which, being closed under convolution, allow for straightforward pricing simulation procedures.

The purpose of this paper is twofold. First, we investigate marginal distributions and correlation structure in the $\rho\alpha$ models. This analytical study shows how the range of the correlation spanned by the model is linked to the process marginal distributions. By calibrating the model, we empirically confirm a trade-off between marginal and correlation fit, as observed in Guillaume (2012) and Luciano *et al* (2016). In particular, a joint calibration of the marginal distributions and the correlation structure may be required to obtain an accurate overall fit.

Second, we examine the pricing performance of $\rho\alpha$ models with regard to barrier reverse convertibles, one of the most popular segments of the Swiss market. A sensitivity analysis quantifies the impact of model parameters on prices and allows us to assess the relative importance of the dependence structure and the marginal processes, given the characteristics in terms of barrier and maturity of contract. Accordingly, the joint calibration procedure can then be fine-tuned to the specific contract's features. Market and model prices are analyzed, and any discrepancies are highlighted and explained.

The structure of this paper is as follows. In Section 2, we describe the structure and characteristics of a typical (multi)barrier reverse convertible as well as the pricing model. Sections 3 and 4 present the theoretical multivariate model and its specifications in terms of the VG and NIG subclasses. The data set is described in Section 5. Section 6 is devoted to model calibration. Section 7 presents a sensitivity analysis, while Section 8 shows the empirical results. Section 9 concludes.

2 MULTIBARRIER REVERSE CONVERTIBLE: MARKET AND FEATURES

The Swiss market for structured financial products is one of the largest in the world, providing us with the opportunity to study complex financial products. Very popular structured products on the Swiss market are MBRCs. Each day, about 4000 MBRCs are listed on the SIX Swiss Exchange, the principal Swiss stock exchange. Among the main issuers are Bank Julius Bär, Bank Vontobel, Banque Cantonale Vaudoise, Credit Suisse, Leonteq Securities, Notenstein La Roche Privatbank, Union Bank of Switzerland (UBS) and Zürcher Kantonalbank.

MBRCs are yield-enhancing products. The investor gives up the capital protection in exchange for high coupons. More specifically, MBRCs offer the investor a high coupon rate during their lifetime, while, according to the price evolution of a basket of underlying assets, we may see different scenarios at maturity. If none of the prices of the underlying assets has hit a downside barrier, or if all the final prices are above their initial fixed levels, the investor will receive 100% of the principal. Otherwise, the investor will receive a given number of shares from the worst-performing stock. The conversion ratio is calculated such that the product of the initial fixing level of any underlying and the conversion ratio is equal to 100. The payoff is illustrated in Figure 1.

Let $\boldsymbol{S} = \{\boldsymbol{S}(t),\ t \geqslant 0\}$ be a price process with n components. Suppose that $S_j(0) = S(0) = 100$ for all $j = 1, \ldots, n$ (this assumption is consistent with the conversion feature explained above), and that $\boldsymbol{B} = (B_1, B_2, \ldots, B_n)$ is a vector of barrier levels. Define $\underline{S}_j(T) = \inf\{S_j(t),\ 0 \leqslant t \leqslant T\}$ and let A be the event that none of the barriers have been broken, that is,

$$A = \bigcap_{j=1}^{n} \{\underline{S}_j(T) > B_j\}.$$

Then, the payoff at maturity T can be written in compact form as

$$100 - 100\left(1 - \min_j \left(\frac{S_j(T)}{S(0)}\right)\right)^{+} \mathbf{1}_{\{A^c\}}, \tag{2.1}$$

FIGURE 1 MBRC payoff at maturity.

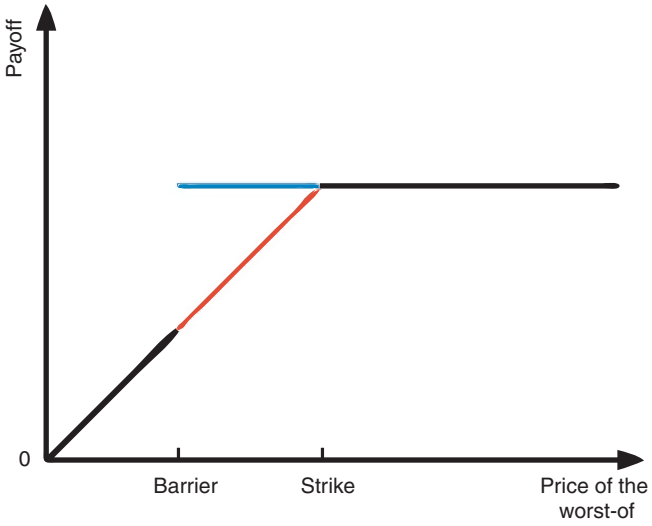

The red line depicts a case in which the barrier has been triggered; the blue line depicts a case where the barrier has not been triggered.

where A^c is the complement of A. From (2.1), it is easy to see that the product can be represented as a portfolio consisting of a long position in a bond and a short position in a worst-of European put with down-and-in feature.

3 FACTOR-BASED SUBORDINATED BROWNIAN MOTIONS

This section recalls the $\rho\alpha$ models introduced in Luciano and Semeraro (2010). Their specifications with the VG and NIG marginal processes are summarized in the online appendix.

The $\rho\alpha$ models are factor-based subordinated Brownian motions constructed as the sum of two independent subordinated Brownian motions. The first has independent components, while the second is a Brownian motion with correlated marginal processes that are subordinated by a common subordinator.

Formally, let $\boldsymbol{B}$ be an n-dimensional Brownian motion with independent components and a Lévy triplet $(\boldsymbol{\mu}, \Sigma, 0)$:

$$\Sigma = \operatorname{diag}(\sigma_1^2, \ldots, \sigma_n^2) := \begin{pmatrix} \sigma_1^2 & 0 & \cdots & 0 \\ 0 & \sigma_2^2 & \cdots & 0 \\ 0 & 0 & \cdots & \sigma_n^2 \end{pmatrix}, \qquad \boldsymbol{\mu} = (\mu_1, \ldots, \mu_n).$$

Let $\boldsymbol{B}^\rho$ be a correlated n-dimensional Brownian motion, with correlations ρ_{ij}, marginal drifts $\boldsymbol{\mu}^\rho = (\mu_1\alpha_1, \ldots, \mu_n\alpha_n)$ and diffusion matrix

$$\Sigma^\rho := \begin{pmatrix} \sigma_1^2\alpha_1 & \rho_{12}\sigma_1\sigma_2\sqrt{\alpha_1}\sqrt{\alpha_2} & \cdots & \rho_{1n}\sigma_1\sigma_n\sqrt{\alpha_1}\sqrt{\alpha_n} \\ \rho_{12}\sigma_1\sigma_2\sqrt{\alpha_1}\sqrt{\alpha_2} & \sigma_2^2\alpha_2 & \cdots & \rho_{2n}\sigma_2\sigma_n\sqrt{\alpha_2}\sqrt{\alpha_n} \\ \vdots & \vdots & \ddots & \vdots \\ \rho_{1n}\sigma_1\sigma_n\sqrt{\alpha_1}\sqrt{\alpha_n} & \rho_{2n}\sigma_2\sigma_n\sqrt{\alpha_2}\sqrt{\alpha_n} & \cdots & \sigma_n^2\alpha_n \end{pmatrix}. \tag{3.1}$$

The $\mathbb{R}^n$-valued subordinated process $\boldsymbol{Y} = \{\boldsymbol{Y}(t),\ t > 0\}$, defined by

$$\boldsymbol{Y}(t) = \begin{pmatrix} B_1(X_1(t)) + B_1^\rho(Z(t)) \\ \cdots \\ B_n(X_n(t)) + B_n^\rho(Z(t)) \end{pmatrix}, \tag{3.2}$$

is a factor-based subordinated Brownian motion, also indicated as the $\rho\alpha$ model. We assume that X_j and Z are independent subordinators, which are also independent of $\boldsymbol{B}$ and $\boldsymbol{B}^\rho$.

Obviously, whenever all the parameters ρ_{ij} collapse to 0 across the different components (that is, $\rho_{ij} = 0$ for $i \neq j$, and $\rho_{ij} = 1$ for $i = j$), we have a version of the model in which the Brownian motions are independent. This version was introduced in Semeraro (2008) and is named the α model.

Luciano and Semeraro (2010, Theorem 5.1) proved that each marginal return j is a Brownian motion with parameters μ_j and σ_j subordinated by the jth marginal process $G_j(t)$ of a factor-based subordinator $\boldsymbol{G}(t)$. A multidimensional factor-based subordinator $\{\boldsymbol{G}(t),\ t \geqslant 0\}$ is defined as follows:

$$\boldsymbol{G}(t) = (X_1(t) + \alpha_1 Z(t), \ldots, X_n(t) + \alpha_n Z(t)), \quad \alpha_j > 0,\ j = 1, \ldots, n,$$

where $\boldsymbol{X}(t) = \{(X_1(t), \ldots, X_n(t)),\ t \geqslant 0\}$ and $\{Z(t),\ t \geqslant 0\}$ are independent subordinators with zero drift, and $\boldsymbol{X}(t)$ has independent components. They represent both the idiosyncratic and common factors of trading activity. Indeed, the following equality in law holds:

$$\mathcal{L}(Y_j(t)) = \mathcal{L}(\mu_j G_j(t) + \sigma_j W(G_j(t))).$$

The marginal laws of $\boldsymbol{Y}(t)$ are, therefore, one-dimensional subordinated Brownian motions. Correlations in the $\rho\alpha$ models are given by

$$\begin{aligned} \rho_{\boldsymbol{Y}}(i,j) &= \frac{\mathrm{Cov}(B_i^\rho, B_j^\rho)E(Z) + E(B_i^\rho)E(B_j^\rho)V(Z)}{\sqrt{V(Y_i)V(Y_j)}} \\ &= \frac{\rho_{ij}\sigma_i\sigma_j\sqrt{\alpha_i}\sqrt{\alpha_j}E(Z) + \mu_i\mu_j\alpha_i\alpha_j V(Z)}{\sqrt{V(Y_i)V(Y_j)}}. \end{aligned}$$

The following equation shows that correlation in these models is higher than in the α models, ie, the submodels with independent Brownian motions:

$$\rho_{\boldsymbol{Y}}(i,j) = \frac{\rho_{ij}\sigma_i\sigma_j\sqrt{\alpha_i}\sqrt{\alpha_j}E(Z)}{\sqrt{V(Y_i)V(Y_j)}} + \rho_{\boldsymbol{Y}_\alpha}(i,j),$$

where $\rho_{\boldsymbol{Y}_\alpha}(i,j)$ are the correlations of the α models. They are independent of time and increasing in α_i, α_j. In particular, if $\alpha_{\boldsymbol{M}} = \max_{j\in\{i,\ldots,n\}}\{\alpha_j\}$, it holds that

$$\rho_{\boldsymbol{Y}}(i,j) \leqslant \frac{\alpha_{\boldsymbol{M}}\sigma_i\sigma_j E(Z) + \alpha_{\boldsymbol{M}}^2\mu_i\mu_j V(Z)}{\sqrt{V(Y_i)V(Y_j)}}.$$

This is true in general. However, the convolution conditions required to recover VG and NIG marginal distributions link the weight parameters α_j with the common subordinator parameters, thus changing the role of α_j. Section 4 discusses the role of α_j for each of the two model specifications with VG and NIG marginal distributions (both of which are introduced in the online appendix).

4 CORRELATION STRUCTURE

In this section, we discuss the correlation structures of the VG and NIG marginal specifications. These are obtained using subordinators with different distributions, as is recalled in the online appendix.

4.1 Variance gamma marginal distributions

We now discuss the correlation structure of the VG specification, $\rho\alpha\,\mathrm{VG}(\boldsymbol{\mu}, \boldsymbol{\alpha}, \boldsymbol{\sigma}, a, \boldsymbol{\rho})$. Linear correlations are

$$\rho_{\boldsymbol{Y}}(i,j) = \frac{(\mu_i\alpha_i\mu_j\alpha_j + \rho_{ij}\sigma_i\sqrt{\alpha_i}\sigma_j\sqrt{\alpha_j})}{\sqrt{(\sigma_i^2 + \mu_i^2\alpha_i)(\sigma_j^2 + \mu_j^2\alpha_j)}}a.$$

They are increasing in a, which satisfies the constraint

$$0 < a < \min_j\left(\frac{1}{\alpha_j}\right).$$

This, depending on $\alpha_{\boldsymbol{M}} = \max_{j\in\{1,\ldots,n\}}\{\alpha_j\}$, provides a bound for admissible correlations, as shown below:

$$\rho_{\boldsymbol{Y}}(i,j) < \frac{\mu_i\mu_j\alpha_i\alpha_j + \rho_{ij}\sigma_i\sigma_j\sqrt{\alpha_i}\sqrt{\alpha_j}}{\sqrt{(\sigma_i^2 + \mu_i^2\alpha_i)(\sigma_j^2 + \mu_j^2\alpha_j)}}\frac{1}{\alpha_{\boldsymbol{M}}}.$$

REMARK 4.1 Suppose $\alpha_j = \alpha$ for all j (as discussed in Leoni and Schoutens (2008)). The inequality in (4.1) becomes

$$\rho_{\boldsymbol{Y}}(i,j) < \frac{\mu_i\mu_j\alpha + \rho_{ij}\sigma_i\sigma_j}{\sqrt{(\sigma_i^2 + \mu_i^2\alpha)(\sigma_j^2 + \mu_j^2\alpha)}}.$$

It can be shown that the upper bound for $\rho_{\boldsymbol{Y}}(i,j)$ depends on α and, in particular, it is increasing in α if

$$\alpha > \frac{\sigma_i\sigma_j(\rho_{ij}\mu_i^2\sigma_j^2 - 2\mu_i\mu_j\sigma_i\sigma_j + \rho_{ij}\mu_j^2\sigma_i^2)}{\mu_i^3\mu_j\sigma_j^2 - 2\rho_{ij}\mu_i^2\mu_j^2\sigma_i\sigma_j + \mu_i\mu_j^3\sigma_i^2},$$

and decreasing otherwise.

The parameter α_j is linked with kurtosis k_{Y_j} of process Y_j and kurtosis k_{G_j} of subordinator G_j. Further, the latter is dominated by the former, being

$$k_{Y_j} = 3(1 + 2\alpha_j - \alpha_j\sigma_j^4(\sigma_j^2 + \alpha_j\mu_j^2)^{-2}) < 3(1 + 2\alpha_j) = k_{G_j}.$$

As a consequence, the asset with the highest α_j drives the maximum correlation achievable. This implies a trade-off between the fit of marginal kurtosis and the range of model-admissible correlations.

If we consider the symmetric case by setting $\mu_i = \mu_j = 0$, we obtain

$$\rho_{\boldsymbol{Y}}(i,j) < \rho_{ij}\sqrt{\frac{\alpha_i}{\alpha_M}}\sqrt{\frac{\alpha_j}{\alpha_M}}.$$

We note that, in this case, the bound does not depend on the kurtosis level, but rather on the range spanned by the kurtosis coefficients of different marginal distributions. More generally, we conclude that the upper bound for the correlation coefficients depends crucially not only on the maximum kurtosis level, but also on the kurtosis range.

The VG process has a gamma subordinator $G(t)$ that satisfies the assumption $E[G(t)] = t$; this lets stochastic time pass like real time in mean. We preserve this assumption for each marginal subordinator in the construction above. By doing so, we impose a constraint on the subordinator parameters. Since the VG process is the only process to have this restriction, we now remove this assumption to see if the trade-off between marginal kurtosis and correlation still remains.

Let $\alpha_j, \lambda_j \in \mathbb{R}^+$ and let a be such that $0 < a < \lambda_j$. Let $\mathcal{L}(X_j) = \Gamma(\lambda_j - a, 1/\alpha_j)$ and $\mathcal{L}(Z) = \Gamma(a,1)$, and assume that X_j, $j = 1,\ldots,n$, and Z are independent random variables. Then, the random vector $\boldsymbol{W}$, defined as

$$\boldsymbol{W} = (W_1, W_2, \ldots, W_n)^{\mathrm{T}} = (X_1 + \alpha_1 Z, X_2 + \alpha_2 Z, \ldots, X_n + \alpha_n Z)^{\mathrm{T}},$$

satisfies $\mathcal{L}(W_j) = \Gamma(\lambda_j, 1/\alpha_j)$, $j = 1, \ldots, n$. Further, the Lévy process $\boldsymbol{G} = \{\boldsymbol{G}(t),\ t \geqslant 0\}$ associated with the distribution of $\boldsymbol{W}$,

$$\mathcal{L}(G_j(t)) = \Gamma\left(\lambda_j t, \frac{1}{\alpha_j}\right), \quad j = 1, \ldots, n,$$

is a multivariate subordinator with marginal gamma distributions. Since the kurtosis of G_j is equal to $3(1 + 2\lambda_j^{-1})$, parameter λ_j drives the subordinator's kurtosis. With this specification of $\boldsymbol{G}$, the process $\boldsymbol{Y}$ is of VG type, with marginal processes of VG type and four parameters $(\mu_j, \sigma_j, \alpha_j, \lambda_j)$.

Return correlations become

$$\rho_{\boldsymbol{Y}}(i, j) = \frac{\rho_{ij}\sigma_i\sigma_j\sqrt{\alpha_i}\sqrt{\alpha_j} + \mu_i\mu_j\alpha_i\alpha_j}{\sqrt{\sigma_j^2\lambda_j\alpha_j + \mu_j^2\alpha_j^2\lambda_j}\sqrt{\sigma_i^2\lambda_i\alpha_i + \mu_i^2\alpha_i^2\lambda_i}}\, a.$$

In this case, the convolution condition implies that the bound for a is given by $a < \lambda_m$, where $\lambda_m = \min_{j\in\{1,\ldots,n\}}\{\lambda_j\}$. The following inequality holds:

$$\begin{aligned}\rho_{\boldsymbol{Y}}(i, j) &< \frac{\rho_{ij}\sigma_i\sigma_j\sqrt{\alpha_i}\sqrt{\alpha_j} + \mu_i\mu_j\alpha_i\alpha_j}{\sqrt{\sigma_j^2\lambda_j\alpha_j + \mu_j^2\alpha_j^2\lambda_j}\sqrt{\sigma_i^2\lambda_i\alpha_i + \mu_i^2\alpha_i^2\lambda_i}}\,\lambda_m \\ &\leqslant \frac{\rho_{ij}\sigma_i\sigma_j\sqrt{\alpha_i}\sqrt{\alpha_j} + \mu_i\mu_j\alpha_i\alpha_j}{\sqrt{\sigma_j^2\alpha_j + \mu_j^2\alpha_j^2}\sqrt{\sigma_i^2\alpha_i + \mu_i^2\alpha_i^2}}\,\frac{\lambda_m}{\lambda_m^{ij}},\end{aligned}$$

where $\lambda_m^{ij} = \min\{\lambda_i, \lambda_j\}$. With these assumptions, the correlation bound depends on the new parameters λ_j. The parameters λ_j play a role similar to that of $1/\alpha_j$ in the traditional VG specification. In fact, they are linked with the marginal kurtosis of the subordinator and the processes Y_j, since

$$3(1 + 2\lambda_j^{-1} - \lambda_j^{-1}\sigma_j^4(\alpha_j\mu_j^2 + \sigma_j^2)^{-2}) \leqslant 3(1 + 2\lambda_j^{-1}) = k_{G_j}.$$

Therefore, one asset displaying much higher marginal kurtosis than other assets in the same portfolio implies that $\lambda_m \ll \lambda_m^{ij}$. This highlights a trade-off between marginal kurtosis and model correlation. To have high marginal kurtosis, the idiosyncratic component must have low λ_j; however, the correlation parameter a is bounded by the minimum λ_j. Thus, it emerges that the trade-off depends on the convolution condition that provides a bound for the common parameter a. This bound depends on the marginal kurtosis parameters and not on the common component weights α_j. Since the trade-off between marginals and correlation still remains, we decide to use the traditional VG in our application.

4.2 Normal inverse Gaussian marginal distributions

The linear correlations in the $\rho\alpha$NIG specification, $\rho\alpha\text{NIG}(\boldsymbol{\gamma}, \boldsymbol{\beta}, \boldsymbol{\delta}, a, \boldsymbol{\rho})$, are

$$\rho_{\boldsymbol{Y}}(i,j) = \frac{\beta_i(\delta_i^2/\zeta_i^2)\beta_j(\delta_j^2/\zeta_j^2) + \rho_{ij}(\delta_i/\zeta_i)(\delta_j/\zeta_j)}{\sqrt{(\gamma_i^2\delta_i(\gamma_i^2-\beta_i^2)^{-3/2})(\gamma_j^2\delta_j(\gamma_j^2-\beta_j^2)^{-3/2})}}\, a,$$

where $\zeta_j = \delta_j\sqrt{\gamma_j^2-\beta_j^2}$. They are increasing in a and must satisfy the constraint

$$0 < a < \min_j \zeta_j.$$

Thus,

$$\rho_{\boldsymbol{Y}}(i,j) < \frac{(\beta_i(\delta_i^2/\zeta_i^2)\beta_j(\delta_j^2/\zeta_j^2) + \rho_{ij}(\delta_i/\zeta_i)(\delta_j/\zeta_j))}{\sqrt{(\gamma_i^2\delta_i(\gamma_i^2-\beta_i^2)^{-3/2})(\gamma_j^2\delta_j(\gamma_j^2-\beta_j^2)^{-3/2})}}\, \zeta_m, \tag{4.1}$$

where $\zeta_m = \min_j \zeta_j$.

REMARK 4.2 Supposing $\zeta_j = \zeta$ for all j, (4.1) becomes

$$\rho_{\boldsymbol{Y}}(i,j) < \frac{\beta_i\beta_j\delta_i^2\delta_j^2}{\gamma_i\gamma_j} + \frac{\rho_{ij}\delta_i\delta_j\zeta^2}{\gamma_i\gamma_j},$$

that is, increasing in ζ.

Since $\beta^2 \leqslant \gamma^2$ and $1/\sqrt{\alpha_j} = \zeta_j$, the kurtosis of $Y_j(t)$ is bounded by the kurtosis of the subordinator G_j as follows:

$$k_{Y_j} = 3\left(1 + \frac{\gamma_j^2 + 4\beta_j^2}{\delta_j\gamma_j^2\sqrt{\gamma_j^2-\beta^2}}\right) \leqslant 3\left(1+\frac{5}{\zeta_j}\right) = k_{G_j}.$$

As in the VG case, the asset with the highest ζ_j drives the maximum correlation achievable, implying a trade-off between the fit of the marginal kurtosis and the range of admissible model correlations.

If we consider the symmetric case, by setting $\delta_i = \delta_j = 0$, we get

$$\rho_{\boldsymbol{Y}}(i,j) < \rho_{ij}\sqrt{\frac{\zeta_m}{\zeta_i}}\sqrt{\frac{\zeta_m}{\zeta_j}}.$$

As in the VG model, in this case, the bound does not depend on the kurtosis level, but rather on the range spanned by the kurtosis coefficients of the different marginal distributions. Again, we conclude that, also for the NIG specification, the upper bound for the correlation coefficients crucially depends not only on the maximum kurtosis level, but also on the kurtosis range.

5 DATA

As Lindauer and Seiz (2008) pointed out, in the primary market we typically observe significant overpricing, while in the secondary market overpricing tends to decrease and/or disappear; in these markets, other factors seem to be decisive in the valuation of the product. For this reason, in our work we use data coming from the secondary market of MBRCs. From the list of the full 3298 MBRCs that traded on the SIX Swiss Exchange on April 10, 2015, we consider only 1205 products whose underlyings are major Swiss stocks for which Eurex options are available. Implied volatility quotes for Eurex stock options are collected from Bloomberg. The underlyings considered are ABB, Credit Suisse Group, Holcim, Nestlé, Novartis, Compagnie Financière (CF) Richemont, Roche Holding, Swatch, Swisscom, SwissLife, SwissRE, Syngenta and Zurich Financial Services. After that, we require the time to maturity to range from 0.9 to 2.2 years, reducing the number of products to 536. For simplicity and comparability with previous works, we exclude from our data set any MBRC product with early redemption features; this leaves us with 119 products. The maturity range has been divided into four maturity buckets (in years) MB1 $:=$ $[0.90, 1.06]$, MB2 $:=$ $[1.06, 1.43]$, MB3 $:=$ $[1.43, 1.93]$ and MB4 $:=$ $[1.93, 2.20]$ for calibration purposes, as discussed in the next section. Further, we drop another seven products, due to the dearth of option quotes for all underlyings in the specific product's maturity bucket.[1] The final data set consists of 112 MBRCs, with thirty-nine different underlying baskets, and four different maturity buckets. The composition of the baskets and their average historical correlations are presented in Table 1. In our data set, 25% of the products belong to the first maturity bucket, 26% to the second, 46% to the third and 3% to the final maturity bucket. The number of underlyings ranges from two to four, with the majority of products linked to three underlyings. Product characteristics are collected from their term sheets. All the MBRCs included in the data set are without any collateral pledge. The issuers are Bank Julius Bär, J. Safra Sarasin, Bank Vontobel, Banque Cantonale Vaudoise, Credit Suisse, Leonteq Securities, Notenstein La Roche Privatbank, UBS and Zürcher Kantonalbank. Barriers range from 38.65% to 84.56% of stock prices at issuance. The underlying price has crossed the barrier for six out of 112 products before April 10, 2015. Coupon payments are annual or semiannual. The annual coupon rate ranges from 3.00% to 11.30% of the nominal. In Figure 2, we provide detailed data set information about the distance-to-barrier (with respect to the initial barrier) and time-to-maturity distributions as well as the spot prices and dividend yields. These spot prices and dividend yields are taken from Bloomberg.

[1] We require the availability of at least five quotes.

TABLE 1 Composition of the baskets and their average sample correlations.

Basket	Asset 1	Asset 2	Asset 3	Asset 4	Average sample correlation
1	ABB	CS	RocheGS		0.54
2	ABB	Nestlé	RocheGS		0.57
3	ABB	Nestlé	Swatch		0.59
4	ABB	RocheGS	Swatch	SwissRe	0.51
5	ABB	RocheGS	Swatch		0.54
6	ABB	RocheGS	Zurich		0.54
7	ABB	Swatch	Syngenta		0.61
8	CS	Holcim	RocheGS		0.55
9	CS	Nestlé	RocheGS		0.54
10	CS	Nestlé	Swatch		0.56
11	CS	Novartis	Richemont		0.57
12	CS	Richemont	RocheGS		0.54
13	CS	Swisscom	Syngenta		0.29
14	Holcim	ABB	Syngenta		0.60
15	Holcim	Nestlé	SwissRE	ABB	0.56
16	Holcim	Novartis	RocheGS		0.61
17	Holcim	Swisscom	Swatch		0.34
18	Nestlé	Novartis	RocheGS		0.67
19	Nestlé	Novartis	Swisscom	ABB	0.44
20	Nestlé	Novartis	Zurich	RocheGS	0.65
21	Nestlé	Richemont	RocheGS		0.62
22	Nestlé	Richemont	Swatch		0.70
23	Nestlé	Richemont	SwissLife		0.61
24	Nestlé	RocheGS	Syngenta		0.57
25	Nestlé	Swatch	Syngenta		0.63
26	Nestlé	SwissLife	Swisscom	Syngenta	0.41
27	Nestlé	Zurich	RocheGS		0.63
28	Novartis	RocheGS			0.69
29	Richemont	ABB	Swatch		0.68
30	Richemont	ABB	Syngenta		0.62
31	RocheGS	Swatch	Zurich		0.54
32	Swisscom	ABB	Swatch		0.31
33	Swisscom	Swatch	Syngenta		0.30
34	Swisscom	Swatch			0.14
35	SwissLife	SwissRE	Swisscom		0.36
36	SwissLife	SwissRe	Zurich	Swatch	0.37
37	SwissRE	ABB	RocheGS		0.54
38	SwissRE	ABB	Syngenta	Swatch	0.50
39	SwissRE	RocheGS	Swatch		0.48
					0.53

FIGURE 2 The (a) distance-to-barrier distribution, (b) initial time-to-maturity distribution and (c) spot prices and dividend yields used.

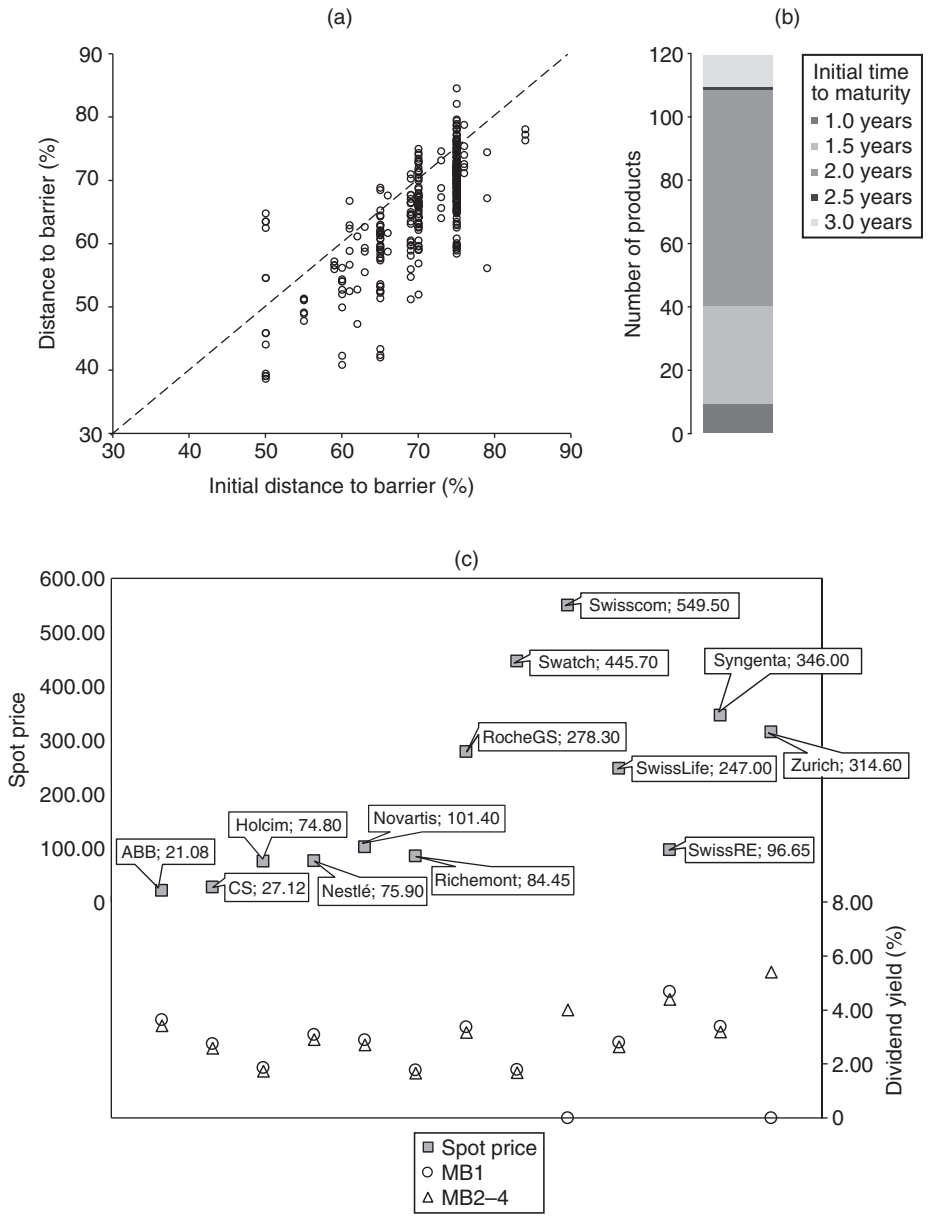

6 CALIBRATION

Define an n-dimensional price process, $\boldsymbol{S} = \{\boldsymbol{S}(t),\ t \geqslant 0\}$, by

$$\boldsymbol{S}(t) = \boldsymbol{S}(0)\exp(\boldsymbol{c}t + \boldsymbol{Y}(t)), \quad \boldsymbol{c} \in \mathbb{R}^n,$$

where $\boldsymbol{c}$ is the compensator and $\boldsymbol{Y}(t)$ is one of the Lévy specifications introduced above.

It is well known that the dependence structure is not necessarily the same under both risk-neutral and historical probability measures; indeed, historical correlations are imperfect proxies for risk-neutral ones, especially during market downturns. Ideally, factor-based Lévy processes should be calibrated to the market prices of MBRCs. However, since closed-form pricing formulas are unlikely to be available for multi-asset exotic derivatives, this is not a feasible approach in practice. Further, other liquid multivariate derivative quotes are not available for our baskets. Thus, we calibrate the correlation structure to historical correlations, as in Luciano and Schoutens (2006) and Leoni and Schoutens (2008).

The $\rho\alpha$ models allow for a two-step calibration. First, we fit marginal parameters to the univariate volatility curves of relevant underlyings for each maturity bucket. Second, we fit common parameters to the sample correlations of the underlying basket. Although this procedure is very appealing, the bound on the common parameter a can restrict the admissible correlation range for the VG and NIG specifications. Therefore, in the spirit of Guillaume (2012), we introduce a joint calibration procedure for each basket of underlyings to enhance the goodness-of-fit of the correlation structure.

6.1 Two-step calibration procedure

Marginal calibration is performed on Eurex settlement data, matching model and market-implied volatilities for each maturity bucket. The total number of calibrations for each model will be 39 baskets $\times$ 4 maturity buckets $=$ 156. Since option quotes are not available for all buckets and underlyings, we are left with thirty-nine calibrations on maturity buckets one and two, twenty calibrations for maturity bucket three, and eight calibrations only for bucket four. For each maturity bucket, we consider only out-of-the-money option quotes with moneyness, defined as $\log S(0)/K$, between -0.60 and 0.60, with a price greater than CHF 0.1. Following Hafner and Wallmeier (2001), for any given underlying, we estimate a smile function for each maturity bucket by cubic interpolation. This procedure allows us to fine-tune the model calibration to the maturity dates of the MBRCs. Risk-free rates are linearly interpolated from the overnight indexed swap (OIS) curve in the corresponding currency. We assume a credit spread of 25 basis points (bps) for issuers whose credit spread is not available in the product's term sheet. Historical correlations, reported in Table 2, are computed on daily log returns over the previous year.

TABLE 2 Sample correlation matrix of daily log returns on underlying assets from April 10, 2009 to April 10, 2010.

	ABB	CS	Holcim	Nestlé	Novartis	Richemont	RocheGS	Swatch	Swisscom	SwissLife	SwissRE	Syngenta	Zurich
ABB	1.000												
CS	0.622	1.000											
Holcim	0.630	0.629	1.000										
Nestlé	0.579	0.513	0.582	1.000									
Novartis	0.593	0.525	0.588	0.712	1.000								
Richemont	0.621	0.558	0.644	0.656	0.634	1.000							
RocheGS	0.510	0.484	0.538	0.612	0.690	0.584	1.000						
Swatch	0.591	0.556	0.632	0.614	0.629	0.817	0.533	1.000					
Swisscom	0.210	0.227	0.260	0.331	0.243	0.140	0.207	0.135	1.000				
SwissLife	0.568	0.605	0.635	0.598	0.621	0.561	0.433	0.546	0.289	1.000			
SwissRE	0.517	0.463	0.547	0.501	0.552	0.499	0.456	0.448	0.246	0.537	1.000		
Syngenta	0.579	0.553	0.602	0.613	0.611	0.652	0.492	0.661	0.090	0.536	0.409	1.000	
Zurich	0.564	0.479	0.576	0.715	0.627	0.609	0.550	0.546	0.296	0.586	0.510	0.530	1.000

Calibration is achieved by minimizing the root mean square error (RMSE) between the model and market implied volatilities, as follows:

$$\mathrm{RMSE} = \sqrt{\frac{1}{N}\sum_{i=1}^{N}(\mathrm{IV}_{\mathrm{mkt}} - \mathrm{IV}_{\mathrm{model}})^2}.$$

We apply the Carr–Madan pricing formula to obtain model prices, and we compute model-implied volatilities by inverting the Black–Scholes formula. We also report the average absolute error (AAE) as an additional goodness-of-fit measure.[2] Thereafter, we calibrate the dependence structure for each basket by minimizing the RMSE between the empirical and the $\rho\alpha$ model return correlations. This yields an estimate of the common parameter a and the Brownian correlations ρ_{ij} for each basket.

6.2 Joint calibration procedure

In this section, we introduce a joint calibration procedure. Setting a given tolerance on the maximum absolute error (MAE) in matching asset correlations, we fit the univariate volatility curves of the underlyings of each basket together. In particular, for each basket of n underlyings, we numerically solve the following problem:

$$\min_{\{\boldsymbol{\theta},a,\boldsymbol{\rho}\}} \sum_{i=1}^{n} \mathrm{RMSE}_i$$
$$\text{such that } \max |\rho_{\boldsymbol{Y}}^{\mathrm{emp}}(j,k) - \rho_{\boldsymbol{Y}}(j,k)| \leqslant \varepsilon,\ j \neq k, \tag{6.1}$$

where $\boldsymbol{\theta}$ is the vector of all marginal parameters, $\boldsymbol{\rho} = \{\rho_{ij}, i = 1,\ldots,n, j = 2,\ldots,n\}$ are the correlation coefficients between the Brownian components collected in $\boldsymbol{B}^{\rho}$, and $\rho_{\boldsymbol{Y}}^{\mathrm{emp}}(i,j)$ and $\rho_{\boldsymbol{Y}}(i,j)$ are the sample and model return correlations, respectively. The threshold ε represents the maximum acceptable level of correlation errors. Setting ε small (at 0.01 or 0.05, for example) ensures an almost perfect replication of the correlation structure, but larger errors in the calibration of the marginal distributions can arise. The relative importance of marginal versus correlation fit can then be fine-tuned through the threshold ε.

6.3 Calibration results

Table 3 shows errors and calibrated marginal parameters for each model, with detailed outputs for the first maturity bucket and summary results for the others. As we can

[2]
$$\mathrm{AAE} = \sum_{i=1}^{N} \frac{|\mathrm{IV}_{\mathrm{mkt}} - \mathrm{IV}_{\mathrm{model}}|}{N}.$$

see, VG and NIG provide a remarkably good fit to the volatility smile. Figure 3 shows volatility goodness-of-fit for maturity bucket one (MB1) and for models VG and NIG for basket eighteen, composed of the three most recurrent underlyings in our data set (see Table 1). The good calibration performance observed is due to the ability of the VG and NIG models to capture skewness and excess kurtosis, yielding a satisfying smile replication for all maturity buckets, with a better fit for the maturity buckets with shorter maturities.

Figure 4 shows the correlation error distribution for the VG and NIG models across all buckets. The correlation error is lower than 0.01 for 53% of baskets in the VG model and 37% of baskets in the NIG model. However, the correlation error is higher than 0.1 for 19% of baskets in the VG model and 41% of baskets in the NIG model.

This result empirically supports the link between the marginal processes and the correlation structure of the multivariate process discussed in Section 4. For both model specifications, the bound on the pairwise correlation depends on the marginal kurtosis of the subordinators obtained in the first step of the calibration. The joint calibration procedure is performed by setting the threshold ε on the correlation fit equal to 0.1 in (6.2) for the baskets that failed to meet this condition in the two-step procedure. Tables 4 and 5 show the ranges of calibrated marginal parameters in the $\rho\alpha$ model specifications for the joint calibration. Marginal fit slightly worsens in the joint calibration procedure with respect to the two-step one. The joint calibration procedure yields an average RMSE of 0.007 for MB1 (compared with the average RMSE of the two-step procedure on the same calibrated underlyings of 0.004), 0.007 for MB2 (compared with 0.009), 0.008 for MB3 (compared with 0.009) and 0.010 for MB4 (compared with 0.010) in the VG case. In the NIG case, the joint calibration procedure yields average RMSEs of 0.005 (compared with 0.005) for MB1, 0.005 (compared with 0.008) for MB2, 0.009 (compared with 0.010) for MB3 and 0.012 (compared with 0.013) for MB4 in the NIG case. While the numerical optimization procedure is straightforward in the VG specification, depending on the kurtosis of the subordinators on parameters α_j only, in the NIG case, the bound depends on $\zeta_j = \delta_j \sqrt{\gamma_j^2 - \beta_j^2}$. In other words, it relies on the interaction of all marginal parameters. How marginal parameters interplay in the multivariate process is examined in more detail in the next section.

7 SENSITIVITY ANALYSIS

In this section, we perform a sensitivity analysis, examining how model parameters affect the value of MBRC products. We consider an MBRC product with two underlyings and typical features: barrier levels are set to 70% of the price of each underlying at issuance, the risk-free rate is 0.25%, the credit spread is 42bps and the dividend yield is 0. We examine two different maturities, six months and one year, and three correlation scenarios, setting the correlation coefficient to 0, 0.25 and 0.75. We define

TABLE 3 Marginal calibration: the first step.

	G	VG					NIG				
MB1	**ATM vol.**	σ	α	μ	**RMSE**	**AAE**	γ	β	δ	**RMSE**	**AAE**
ABB	0.1794	0.1779	0.5379	−0.1466	0.0005	0.0004	11.1637	−6.6745	0.2537	0.0009	0.0008
CS	0.2206	0.2279	0.5586	−0.1439	0.0011	0.0008	6.1235	−2.7808	0.2838	0.0021	0.0018
Holcim	0.2231	0.2272	0.4323	−0.1511	0.0017	0.0015	7.5405	−3.3371	0.3406	0.0023	0.0021
Nestlé	0.1361	0.1398	0.7991	−0.0946	0.0011	0.0009	9.2972	−5.1016	0.1505	0.0014	0.0012
Novartis	0.1728	0.1735	0.3702	−0.1236	0.0010	0.0007	9.6977	−4.0181	0.2674	0.0012	0.0011
Richemont	0.2179	0.2161	0.4620	−0.1699	0.0008	0.0006	9.0647	−4.9368	0.3272	0.0013	0.0011
RocheGS	0.1732	0.1774	0.4077	−0.1112	0.0007	0.0006	9.4336	−3.6025	0.2739	0.0014	0.0013
Swatch	0.2156	0.2180	0.4474	−0.1495	0.0005	0.0004	7.2771	−3.2081	0.3102	0.0012	0.0011
Swisscom	0.1607	0.1665	0.7484	−0.0871	0.0014	0.0013	7.0168	−3.0234	0.1770	0.0017	0.0015
SwissLife	0.1865	0.1892	0.4845	−0.1307	0.0006	0.0005	8.1377	−3.7008	0.2590	0.0013	0.0012
SwissRE	0.1715	0.1737	0.4461	−0.1334	0.0013	0.0011	9.4997	−4.6031	0.2497	0.0019	0.0017
Syngenta	0.1834	0.1829	0.4785	−0.1457	0.0009	0.0007	9.4894	−4.8714	0.2660	0.0019	0.0017
Zurich	0.1695	0.1560	0.4332	−0.1607	0.0028	0.0024	11.9830	−7.0119	0.2335	0.0015	0.0013
					Av. RMSE	**Av. AAE**				**Av. RMSE**	**Av. AAE**
MB1					0.0011	0.0009				0.0016	0.0014
MB2					0.0016	0.0013				0.0013	0.0011
MB3					0.0019	0.0016				0.0023	0.0021
MB4					0.0031	0.0026				0.0036	0.0032

FIGURE 3 Marginal calibration fit on Nestlé, Novartis and RocheGS.

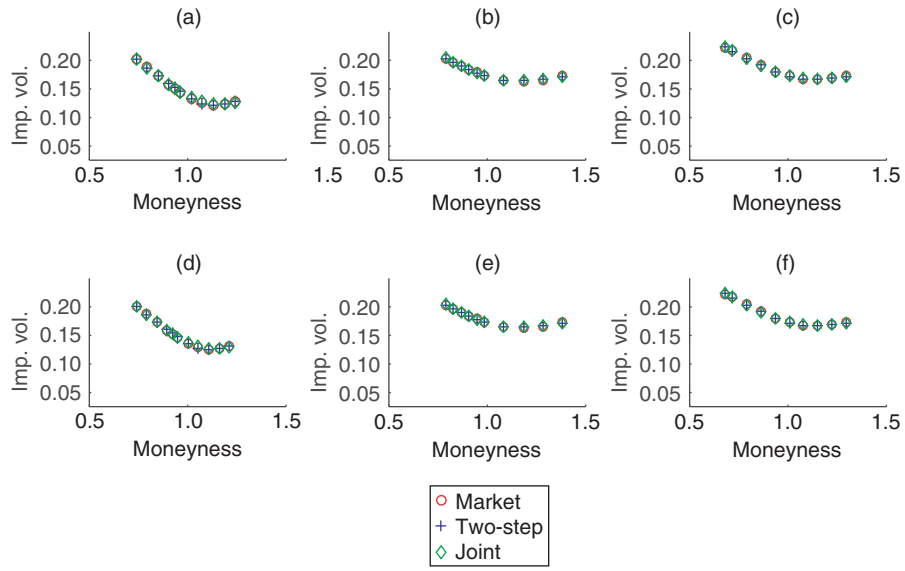

The following cases are depicted: (a) Nestlé with the VG model; (b) Novartis with the VG model; (c) RocheGS with the VG model; (d) Nestlé with the NIG model; (e) Novartis with the NIG model; (f) RocheGS with the NIG model.

a base case, assuming the same marginal distributions for both assets, with parameters chosen consistently with the calibration results of Section 6. Different cases are obtained by either halving or doubling each parameter of the base case. Put prices are expressed as percentages of the base put price. Our analysis shows that the movement of MBRC prices is consistent with changes in the moments of marginal distributions. Below, we discuss put price variations due to changes in marginal moments and correlation. While marginal moments are directly linked with marginal parameters in the VG case, this is not true for the NIG case.

In Table 6, the VG model is considered.[3] The marginal parameters of the base case are $\sigma = 0.230$, $\alpha = 0.377$ and $\mu = 0$ for both marginal processes. We find that the

[3] For Table 6, the marginal parameters are as follows: $\{\sigma_L, \sigma, \sigma_H\} = \{0.115, 0.230, 0.460\}$, $\{\alpha_L, \alpha, \alpha_H\} = \{0.188, 0.377, 0.754\}$, $\{\mu_L, \mu, \mu_H\} = \{-0.252, 0, 0.252\}$. In addition, an asterisk indicates that the correlation level cannot be reached. The base put prices are reported in the top-left corner of panels (a)–(c) and (e)–(f). In each column, we change one marginal parameter of one process, while in each row we change one marginal parameter of the other process. On the main diagonal, the two marginal distributions are identical. The marginal moments corresponding to different parameter sets are shown in panels (d) and (h) of the table.

FIGURE 4 Distribution of the maximum absolute correlation error under the (a) VG and (b) NIG models in the two-step calibration procedure.

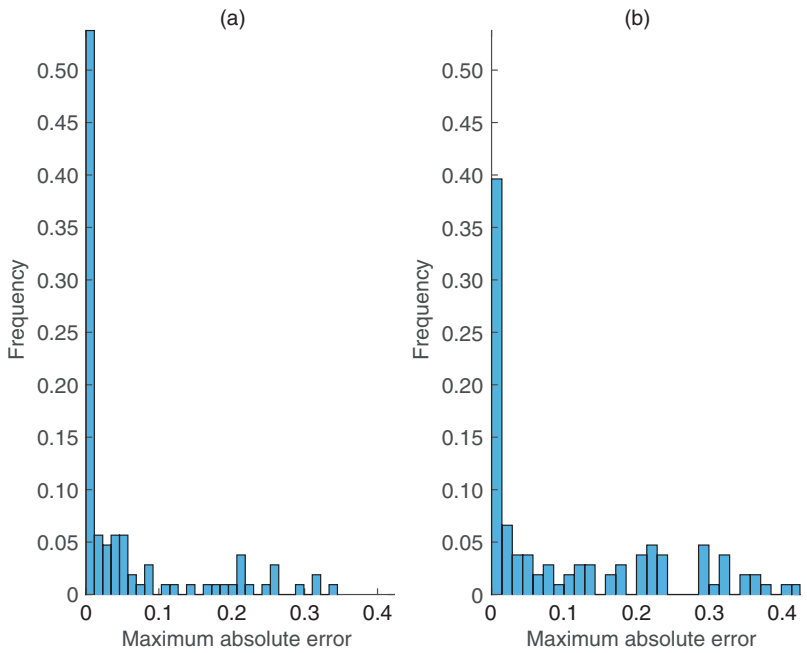

put value increases with the marginal parameter σ, which drives the variance of the marginal distribution. More specifically, if the variance of one marginal distribution increases, the put value is almost insensitive to the variance level of the other marginal, due to the worst-of feature of the product. The effect of the sign of the skewness can be read through the parameter μ. When the skewness parameter moves to negative values, the put price increases (and vice versa). The effect of marginal kurtosis on option prices depends on the time to maturity. We find a direct relationship between kurtosis and the option value for short maturities, and an inverse relationship with long maturities, as observed in Wallmeier and Diethelm (2012). This is one interpretation that may be drawn from Figure 5, which shows the distribution of the minimum for the two scenarios of time to maturity. When parameter α, which mainly controls kurtosis in the VG model, changes from its original level of 0.377 to $\alpha_{\mathrm{L}} = \alpha/2 = 0.188$, both marginal distributions of log returns present six-month kurtosis of 4.1310. In the case of $\alpha_H = 2\alpha = 0.754$, six-month kurtosis raises to 7.5238. However, this implies kurtosis levels for the one-year distributions of 3.5655 and 5.2619. In this analysis, we keep the barrier level constant for both time-to-maturity scenarios. This implies a shift

TABLE 4 Marginal calibration (joint calibration procedure): VG model.

	σ		α		μ		RMSE		AAE		APE		
MB1	**Min**	**Max**	**Min**	**Max**	**Min**	**Max**	**Min**	**Max**	**Min**	**Max**	**Min**	**Max**	**No. of cal.**
ABB													0
CS													0
Holcim													0
Nestlé	0.1383	0.1412	0.6774	0.7364	−0.1038	−0.0931	0.0017	0.0021	0.0015	0.0017	0.0388	0.0412	3
Novartis	0.1735	0.1738	0.4161	0.4666	−0.1175	−0.0988	0.0012	0.0036	0.0011	0.0034	0.0145	0.0346	2
Richemont	0.2192	0.2192	0.5132	0.5132	−0.1565	−0.1565	0.0010	0.0010	0.0007	0.0007	0.0180	0.0180	1
RocheGS	0.1744	0.1776	0.4082	0.4200	−0.1288	−0.1091	0.0008	0.0032	0.0006	0.0028	0.0260	0.0396	2
Swatch	0.2183	0.2183	0.4606	0.4606	−0.1470	−0.1470	0.0006	0.0006	0.0004	0.0004	0.0128	0.0128	1
Swisscom													0
SwissLife													0
SwissRE													0
Syngenta													0
Zurich	0.1496	0.1496	0.3900	0.3900	−0.1711	−0.1711	0.0050	0.0050	0.0040	0.0040	0.0567	0.0567	1

Empty rows correspond to underlyings that belong to baskets with MAE values of lower than 0.1. For each underlying, the last column indicates the number of baskets calibrated with the joint procedure. “APE” denotes average percentage error.

TABLE 5 Marginal calibration (joint calibration procedure): NIG model.

	γ		β		δ		RMSE		AAE		APE		
MB1	**Min**	**Max**	**Min**	**Max**	**Min**	**Max**	**Min**	**Max**	**Min**	**Max**	**Min**	**Max**	**No. of cal.**
ABB	10.6678	11.0661	−6.5984	−6.2858	0.2492	0.2528	0.0009	0.0009	0.0008	0.0008	0.0255	0.0257	2
CS													0
Holcim	7.2368	7.3240	−3.2151	−3.1668	0.3312	0.3339	0.0023	0.0023	0.0021	0.0021	0.0266	0.0266	2
Nestlé	9.3021	11.2089	−6.4066	−5.1032	0.1505	0.1685	0.0014	0.0023	0.0012	0.0018	0.0481	0.0485	7
Novartis	9.2543	10.2738	−4.2669	−3.8554	0.2559	0.2813	0.0013	0.0014	0.0010	0.0012	0.0139	0.0173	3
Richemont	7.4258	8.8555	−4.7838	−3.7852	0.2956	0.3236	0.0013	0.0016	0.0011	0.0011	0.0207	0.0211	2
RocheGS	9.1984	9.4199	−3.6021	−3.4872	0.2682	0.2736	0.0014	0.0015	0.0012	0.0013	0.0333	0.0334	3
Swatch	7.0315	7.2573	−3.1979	−3.0846	0.3019	0.3095	0.0012	0.0013	0.0011	0.0011	0.0172	0.0177	4
Swisscom	7.0747	7.1845	−3.0989	−3.0495	0.1783	0.1806	0.0017	0.0017	0.0014	0.0015	0.0433	0.0438	3
SwissLife													0
SwissRE	9.4840	9.4840	−4.5946	−4.5946	0.2494	0.2494	0.0019	0.0019	0.0017	0.0017	0.0259	0.0259	1
Syngenta	9.3101	9.4756	−4.8630	−4.7539	0.2628	0.2657	0.0019	0.0019	0.0016	0.0017	0.0400	0.0403	2
Zurich	12.3541	12.3541	−7.2705	−7.2705	0.2379	0.2379	0.0015	0.0015	0.0013	0.0013	0.0387	0.0387	1

Empty rows correspond to underlyings that belong to baskets with MAE values of lower than 0.1. For each underlying, the last column indicates the number of baskets calibrated with the joint procedure.

TABLE 6 Sensitivity to marginal parameter changes: VG model. [Table continues on next page.]

(a) Put price, 2.0345; $T = 0.5$, $\rho_Y = 0$

	(σ, α, μ)	$(\sigma_{\mathbf{L}}, \alpha, \mu)$	$(\sigma_{\mathbf{H}}, \alpha, \mu)$	$(\sigma, \alpha_{\mathbf{L}}, \mu)$	$(\sigma, \alpha_{\mathbf{H}}, \mu)$	$(\sigma, \alpha, \mu_{\mathbf{L}})$	$(\sigma, \alpha, \mu_{\mathbf{H}})$
(σ, α, μ)	100.00						
$(\sigma_{\mathbf{L}}, \alpha, \mu)$	54.34	3.28					
$(\sigma_{\mathbf{H}}, \alpha, \mu)$	375.34	334.17	620.74				
$(\sigma, \alpha_{\mathbf{L}}, \mu)$	103.39	51.17	372.56	94.50			
$(\sigma, \alpha_{\mathbf{H}}, \mu)$	105.31	60.23	386.53	104.57	110.88		
$(\sigma, \alpha, \mu_{\mathbf{L}})$	189.25	145.40	448.30	185.59	196.14	281.59	
$(\sigma, \alpha, \mu_{\mathbf{H}})$	80.41	31.72	363.05	76.48	84.02	172.91	53.75

(b) Put price, 1.9730; $T = 0.5$, $\rho_Y = 0.25$

	(σ, α, μ)	$(\sigma_{\mathbf{L}}, \alpha, \mu)$	$(\sigma_{\mathbf{H}}, \alpha, \mu)$	$(\sigma, \alpha_{\mathbf{L}}, \mu)$	$(\sigma, \alpha_{\mathbf{H}}, \mu)$	$(\sigma, \alpha, \mu_{\mathbf{L}})$	$(\sigma, \alpha, \mu_{\mathbf{H}})$
(σ, α, μ)	100.00						
$(\sigma_{\mathbf{L}}, \alpha, \mu)$	54.98	2.83					
$(\sigma_{\mathbf{H}}, \alpha, \mu)$	373.13	349.81	576.90				
$(\sigma, \alpha_{\mathbf{L}}, \mu)$	99.72	51.70	379.87	97.94			
$(\sigma, \alpha_{\mathbf{H}}, \mu)$	103.63	56.68	379.64	100.12	106.28		
$(\sigma, \alpha, \mu_{\mathbf{L}})$	182.76	148.82	422.09	184.69	182.25	265.01	
$(\sigma, \alpha, \mu_{\mathbf{H}})$	76.62	31.98	357.59	74.33	83.30	165.63	54.75

(c) Put price, 1.6097; $T = 0.5$, $\rho_Y = 0.75$

	(σ, α, μ)	$(\sigma_{\mathbf{L}}, \alpha, \mu)$	$(\sigma_{\mathbf{H}}, \alpha, \mu)$	$(\sigma, \alpha_{\mathbf{L}}, \mu)$	$(\sigma, \alpha_{\mathbf{H}}, \mu)$	$(\sigma, \alpha, \mu_{\mathbf{L}})$	$(\sigma, \alpha, \mu_{\mathbf{H}})$
(σ, α, μ)	100.00						
$(\sigma_{\mathbf{L}}, \alpha, \mu)$	66.69	3.60					
$(\sigma_{\mathbf{H}}, \alpha, \mu)$	427.57	422.64	586.70				
$(\sigma, \alpha_{\mathbf{L}}, \mu)$	100.18*	61.32*	436.30*	98.44			
$(\sigma, \alpha_{\mathbf{H}}, \mu)$	110.37*	73.45*	426.89*	122.11*	113.84		
$(\sigma, \alpha, \mu_{\mathbf{L}})$	187.28	174.55	459.97	209.82*	199.20*	254.95	
$(\sigma, \alpha, \mu_{\mathbf{H}})$	82.65	35.15	421.94	77.13*	92.05*	189.86*	56.40

(d) Marginal moments, $T = 0.5$

	(σ, α, μ)	$(\sigma_{\mathbf{L}}, \alpha, \mu)$	$(\sigma_{\mathbf{H}}, \alpha, \mu)$	$(\sigma, \alpha_{\mathbf{L}}, \mu)$	$(\sigma, \alpha_{\mathbf{H}}, \mu)$	$(\sigma, \alpha, \mu_{\mathbf{L}})$	$(\sigma, \alpha, \mu_{\mathbf{H}})$
$\mathrm{Var}(Y)$	0.0284	0.0071	0.1134	0.0284	0.0284	0.0403	0.0403
$\mathrm{Skew}(Y)$	0.0000	0.0000	0.0000	0.0000	0.0000	−1.2789	1.2789
$\mathrm{Kurt}(Y)$	5.2619	5.2619	5.2619	4.1310	7.5238	6.4056	6.4056

TABLE 6 Continued.

(e) Put price, 6.8241; $T = 1$, $\rho_Y = 0$

	(σ, α, μ)	$(\sigma_{\mathbf{L}}, \alpha, \mu)$	$(\sigma_{\mathbf{H}}, \alpha, \mu)$	$(\sigma, \alpha_{\mathbf{L}}, \mu)$	$(\sigma, \alpha_{\mathbf{H}}, \mu)$	$(\sigma, \alpha, \mu_{\mathbf{L}})$	$(\sigma, \alpha, \mu_{\mathbf{H}})$
(σ, α, μ)	100.00						
$(\sigma_{\mathbf{L}}, \alpha, \mu)$	53.14	5.35					
$(\sigma_{\mathbf{H}}, \alpha, \mu)$	250.49	218.38	376.15				
$(\sigma, \alpha_{\mathbf{L}}, \mu)$	102.69	57.92	255.26	103.12			
$(\sigma, \alpha_{\mathbf{H}}, \mu)$	95.72	50.26	250.75	98.79	91.65		
$(\sigma, \alpha, \mu_{\mathbf{L}})$	140.58	98.64	284.49	141.41	137.28	175.17	
$(\sigma, \alpha, \mu_{\mathbf{H}})$	107.30	65.96	259.97	113.40	105.20	148.25	120.99

(f) Put price, 6.0863; $T = 1$, $\rho_Y = 0.25$

	(σ, α, μ)	$(\sigma_{\mathbf{L}}, \alpha, \mu)$	$(\sigma_{\mathbf{H}}, \alpha, \mu)$	$(\sigma, \alpha_{\mathbf{L}}, \mu)$	$(\sigma, \alpha_{\mathbf{H}}, \mu)$	$(\sigma, \alpha, \mu_{\mathbf{L}})$	$(\sigma, \alpha, \mu_{\mathbf{H}})$
(σ, α, μ)	100.00						
$(\sigma_{\mathbf{L}}, \alpha, \mu)$	60.86	6.21					
$(\sigma_{\mathbf{H}}, \alpha, \mu)$	272.94	243.99	385.26				
$(\sigma, \alpha_{\mathbf{L}}, \mu)$	106.47	64.67	273.41	111.08			
$(\sigma, \alpha_{\mathbf{H}}, \mu)$	98.90	55.99	267.70	103.29	92.66		
$(\sigma, \alpha, \mu_{\mathbf{L}})$	140.66	110.45	294.48	147.81	137.92	182.11	
$(\sigma, \alpha, \mu_{\mathbf{H}})$	116.41	73.02	277.59	118.92	113.98	152.96	129.97

(g) Put price, 5.1856; $T = 1$, $\rho_Y = 0.75$

	(σ, α, μ)	$(\sigma_{\mathbf{L}}, \alpha, \mu)$	$(\sigma_{\mathbf{H}}, \alpha, \mu)$	$(\sigma, \alpha_{\mathbf{L}}, \mu)$	$(\sigma, \alpha_{\mathbf{H}}, \mu)$	$(\sigma, \alpha, \mu_{\mathbf{L}})$	$(\sigma, \alpha, \mu_{\mathbf{H}})$
(σ, α, μ)	100.00						
$(\sigma_{\mathbf{L}}, \alpha, \mu)$	66.47	6.20					
$(\sigma_{\mathbf{H}}, \alpha, \mu)$	293.43	280.18	379.43				
$(\sigma, \alpha_{\mathbf{L}}, \mu)$	107.59*	74.25*	298.61*	108.95			
$(\sigma, \alpha_{\mathbf{H}}, \mu)$	97.83*	64.56*	288.90*	114.62*	89.75		
$(\sigma, \alpha, \mu_{\mathbf{L}})$	135.16	127.00	308.76	156.31*	145.55*	173.06	
$(\sigma, \alpha, \mu_{\mathbf{H}})$	113.31	81.99	293.19	124.94*	119.06*	171.56*	128.44

(h) Marginal moments, $T = 1$

	(σ, α, μ)	$(\sigma_{\mathbf{L}}, \alpha, \mu)$	$(\sigma_{\mathbf{H}}, \alpha, \mu)$	$(\sigma, \alpha_{\mathbf{L}}, \mu)$	$(\sigma, \alpha_{\mathbf{H}}, \mu)$	$(\sigma, \alpha, \mu_{\mathbf{L}})$	$(\sigma, \alpha, \mu_{\mathbf{H}})$
$\mathrm{Var}(Y)$	0.0567	0.0142	0.2268	0.0567	0.0567	0.0806	0.0806
$\mathrm{Skew}(Y)$	0.0000	0.0000	0.0000	0.0000	0.0000	−0.9043	0.9043
$\mathrm{Kurt}(Y)$	4.1310	4.1310	4.1310	3.5655	5.2619	4.7028	4.7028

in the distribution of the minimum of the two assets at maturity without a shift in the barrier; thus, the probability of hitting the barrier changes by construction. As one may observe in Figure 5, the probability of hitting the barrier is very similar in Figures 5(a), 5(c) and 5(e), with a slightly higher probability in the case of high kurtosis. On the contrary, in the case with one-year maturity, the probability of hitting the barrier is higher when the kurtosis is lower, as in Figures 5(b), 5(d) and 5(f). We then observe different effects of the marginal distributions kurtosis, depending on the combination of barrier levels and the maturity of the product. In particular, the more significantly the barrier level differs from the strike price, the more significantly a direct relation between kurtosis and put value is magnified. This is because the hitting event will depend increasingly on the heaviness of the left tail of the distribution. Barriers very close to the strike price, however, increase the probability of the hitting event in the case of more platykurtic marginal distributions. Of course, a strong positive correlation implies lower put values for both short and long maturities. In our simulation, the VG model can recover a correlation level of 0.75 among the marginal processes in nine cases out of twenty-one possible combinations of marginal parameters.

Table 7 shows sensitivity results for the NIG model.[4] The base case has marginal parameters $\gamma = 7.15$, $\beta = 0$ and $\delta = 0.378$. We note that the option value in the case of independence between marginal processes and short maturity is very similar to the VG price, since the marginal processes present almost identical moments up to the fourth one. The moments of the NIG process cannot be moved by changing a single parameter, which is in direct contrast to the VG setting. In the symmetric case, however, we can overcome this limitation by moving along the main diagonal of each panel, that is, by considering processes with the same marginal distribution. In fact, we can find a certain parameter combination that allows us to move only one moment at a time.[5] From Table 7, it emerges that the effect on the put value of a change in

[4] In Table 7, the marginal parameters used in the sensitivity analysis are as follows:

$$\{\gamma_{\mathrm{L}}, \gamma, \gamma_{\mathrm{H}}\} = \{3.575, 7.150, 14.300\},$$
$$\{\beta_{\mathrm{L}}, \beta, \beta_{\mathrm{H}}\} = \{-2.500, 0.000, 2.500\},$$
$$\{\delta_{\mathrm{L}}, \delta, \delta_{\mathrm{H}}\} = \{0.189, 0.378, 0.756\}.$$

In addition, an asterisk indicates that the correlation level cannot be reached. The base put prices are reported in the top-left corner of panels (a)–(c) and (e)–(f). In each column, we change one marginal parameter of one process, while in each row we change one marginal parameter of the other process. On the main diagonal, the two marginal distributions are identical. The marginal moments corresponding to different parameter sets are shown in panels (d) and (h) of the table.

[5] For instance, compare two different cases along the main diagonal: $(0, 2\gamma, \delta)$ and $(0, \gamma, 2\delta)$ for both marginal processes. They have different marginal variances, and the same skewness and kurtosis. In fact, we have $V(Y) = \delta/(2\gamma)$ in the first case and $V(Y) = 2\delta/\gamma$ in the second, while kurtosis is $k_Y = 3(1 + 1/2\delta\gamma)$ in both cases. The same applies for $(0, \gamma/2, \delta)$ and $(0, \gamma, \delta/2)$. To have

FIGURE 5 Distribution of the minimum of log returns at maturity with the VG model.

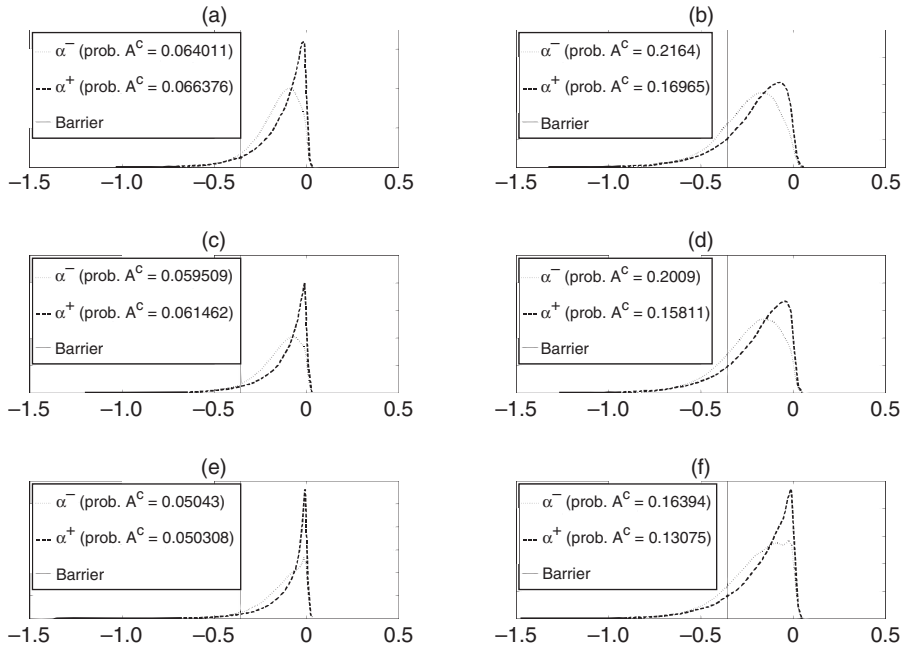

(a) Six months, $\rho_Y = 0$. (b) One year, $\rho_Y = 0$. (c) Six months, $\rho_Y = 0.25$. (d) One year, $\rho_Y = 0.25$. (e) Six months, $\rho_Y = 0.75$. (f) One year, $\rho_Y = 0.75$.

the marginal variances depends on the kurtosis levels of the marginal distributions. Further, we observe the same relationship between kurtosis and option value as in the VG model. As with μ in the VG economy, changing the β parameter has a direct effect on the skewness of marginal distributions, with an inverse relation with respect to the worst-of put value. A correlation level of 0.75 can be recovered in six out of twenty-one possible combinations of marginal parameters.

Finally, Figure 6 shows the sensitivity of put prices to different correlation levels for our base case.

8 PRICING

Since no analytical pricing formula is available, we price the MBRCs of our data set via Monte Carlo simulation, with daily time steps and 2^{17} paths. The time-change

different marginal kurtosis and the same variances and skewness, we may consider, for instance, $(0, 2\gamma, \delta)$ and $(0, \gamma, \delta/2)$ for both marginal processes.

TABLE 7 Sensitivity to marginal parameter changes: NIG model. [Table continues on next page.]

(a) Put price, 2.0356; $T = 0.5$, $\rho_Y = 0$

	(γ, β, δ)	$(\gamma_L, \beta, \delta)$	$(\gamma_H, \beta, \delta)$	$(\gamma, \beta_L, \delta)$	$(\gamma, \beta_H, \delta)$	$(\gamma, \beta, \delta_L)$	$(\gamma, \beta, \delta_H)$
(γ, β, δ)	100.00						
$(\gamma_L, \beta, \delta)$	188.16	269.71					
$(\gamma_H, \beta, \delta)$	56.42	143.31	17.34				
$(\gamma, \beta_L, \delta)$	145.78	225.28	99.61	194.38			
$(\gamma, \beta_H, \delta)$	81.46	170.89	42.26	132.98	71.31		
$(\gamma, \beta, \delta_L)$	64.27	150.40	24.66	109.99	52.19	29.04	
$(\gamma, \beta, \delta_H)$	208.78	285.65	173.43	254.49	198.17	179.41	311.18

(b) Put price 1.8406; $T = 0.5$, $\rho_Y = 0.25$

	(γ, β, δ)	$(\gamma_L, \beta, \delta)$	$(\gamma_H, \beta, \delta)$	$(\gamma, \beta_L, \delta)$	$(\gamma, \beta_H, \delta)$	$(\gamma, \beta, \delta_L)$	$(\gamma, \beta, \delta_H)$
(γ, β, δ)	100.00						
$(\gamma_L, \beta, \delta)$	196.75	271.40					
$(\gamma_H, \beta, \delta)$	61.22	157.71	17.77				
$(\gamma, \beta_L, \delta)$	146.64	236.04	108.04	188.68			
$(\gamma, \beta_H, \delta)$	92.82	177.46	50.33	132.88	73.15		
$(\gamma, \beta, \delta_L)$	63.98	162.27	24.67	118.44	56.22	33.30	
$(\gamma, \beta, \delta_H)$	215.83	303.89	188.98	257.50	207.85	188.19	325.53

(c) Put price 1.5166; $T = 0.5$, $\rho_Y = 0.75$

	(γ, β, δ)	$(\gamma_L, \beta, \delta)$	$(\gamma_H, \beta, \delta)$	$(\gamma, \beta_L, \delta)$	$(\gamma, \beta_H, \delta)$	$(\gamma, \beta, \delta_L)$	$(\gamma, \beta, \delta_H)$
(γ, β, δ)	100.00						
$(\gamma_L, \beta, \delta)$	68.01*	270.20					
$(\gamma_H, \beta, \delta)$	12.15*	11.94*	17.44				
$(\gamma, \beta_L, \delta)$	142.99	128.89*	11.44	186.98			
$(\gamma, \beta_H, \delta)$	90.59	46.35*	10.18*	135.38	76.09		
$(\gamma, \beta, \delta_L)$	67.75*	188.90	11.75*	132.24*	48.26*	30.50	
$(\gamma, \beta, \delta_H)$	209.19*	216.71*	221.84	220.71*	224.16*	209.07*	330.53

(d) Marginal moments, $T = 0.5$

	(γ, β, δ)	$(\gamma_L, \beta, \delta)$	$(\gamma_H, \beta, \delta)$	$(\gamma, \beta_L, \delta)$	$(\gamma, \beta_H, \delta)$	$(\gamma, \beta, \delta_L)$	$(\gamma, \beta, \delta_H)$
$\mathrm{Var}(Y)$	0.0264	0.0529	0.0132	0.0321	0.0321	0.0132	0.0529
$\mathrm{Skew}(Y)$	0.0000	0.0000	0.0000	−0.9322	0.9322	0.0000	0.0000
$\mathrm{Kurt}(Y)$	5.2200	7.4400	4.1100	6.5283	6.5283	7.4400	4.1100

TABLE 7 Continued.

(e) Put price 6.5146; $T = 1$, $\rho_Y = 0$

	(γ, β, δ)	$(\gamma_L, \beta, \delta)$	$(\gamma_H, \beta, \delta)$	$(\gamma, \beta_L, \delta)$	$(\gamma, \beta_H, \delta)$	$(\gamma, \beta, \delta_L)$	$(\gamma, \beta, \delta_H)$
(γ, β, δ)	100.00						
$(\gamma_L, \beta, \delta)$	149.97	205.14					
$(\gamma_H, \beta, \delta)$	64.38	122.64	27.73				
$(\gamma, \beta_L, \delta)$	117.43	177.87	86.02	140.51			
$(\gamma, \beta_H, \delta)$	100.37	158.16	65.78	121.92	102.42		
$(\gamma, \beta, \delta_L)$	64.75	125.55	30.04	86.63	66.30	30.56	
$(\gamma, \beta, \delta_H)$	169.43	220.00	144.28	191.18	173.07	143.49	236.56

(f) Put price 5.8367; $T = 1$, $\rho_Y = 0.25$

	(γ, β, δ)	$(\gamma_L, \beta, \delta)$	$(\gamma_H, \beta, \delta)$	$(\gamma, \beta_L, \delta)$	$(\gamma, \beta_H, \delta)$	$(\gamma, \beta, \delta_L)$	$(\gamma, \beta, \delta_H)$
(γ, β, δ)	100.00						
$(\gamma_L, \beta, \delta)$	160.05	208.01					
$(\gamma_H, \beta, \delta)$	67.51	132.20	30.50				
$(\gamma, \beta_L, \delta)$	122.32	177.40	93.11	145.26			
$(\gamma, \beta_H, \delta)$	104.75	164.02	74.60	124.42	112.21		
$(\gamma, \beta, \delta_L)$	68.43	133.61	31.30	93.06	74.44	30.98	
$(\gamma, \beta, \delta_H)$	179.98	230.71	154.59	196.11	184.00	153.66	242.81

(g) Put price 4.8473; $T = 1$, $\rho_Y = 0.75$

	(γ, β, δ)	$(\gamma_L, \beta, \delta)$	$(\gamma_H, \beta, \delta)$	$(\gamma, \beta_L, \delta)$	$(\gamma, \beta_H, \delta)$	$(\gamma, \beta, \delta_L)$	$(\gamma, \beta, \delta_H)$
(γ, β, δ)	100.00						
$(\gamma_L, \beta, \delta)$	66.36*	207.65					
$(\gamma_H, \beta, \delta)$	19.00*	18.45*	28.54				
$(\gamma, \beta_L, \delta)$	120.82	100.56*	19.35	140.84			
$(\gamma, \beta_H, \delta)$	104.39	70.95*	19.24	122.04	111.52		
$(\gamma, \beta, \delta_L)$	68.94*	148.81	19.38*	101.56*	71.38*	31.24	
$(\gamma, \beta, \delta_H)$	172.06*	173.55*	177.34	171.11*	172.43*	171.19*	240.77

(h) Marginal moments, $T = 1$

(γ, β, δ)	$(\gamma_L, \beta, \delta)$	$(\gamma_H, \beta, \delta)$	$(\gamma, \beta_L, \delta)$	$(\gamma, \beta_H, \delta)$	$(\gamma, \beta, \delta_L)$	$(\gamma, \beta, \delta_H)$
$\mathrm{Var}(Y)$	0.0529	0.1057	0.0264	0.0643	0.0643	0.0264	0.1057
$\mathrm{Skew}(Y)$	0.0000	0.0000	0.0000	−0.6592	0.6592	0.0000	0.0000
$\mathrm{Kurt}(Y)$	4.1100	5.2200	3.5550	4.7642	4.7642	5.2200	3.5550

FIGURE 6 Sensitivity to correlation changes.

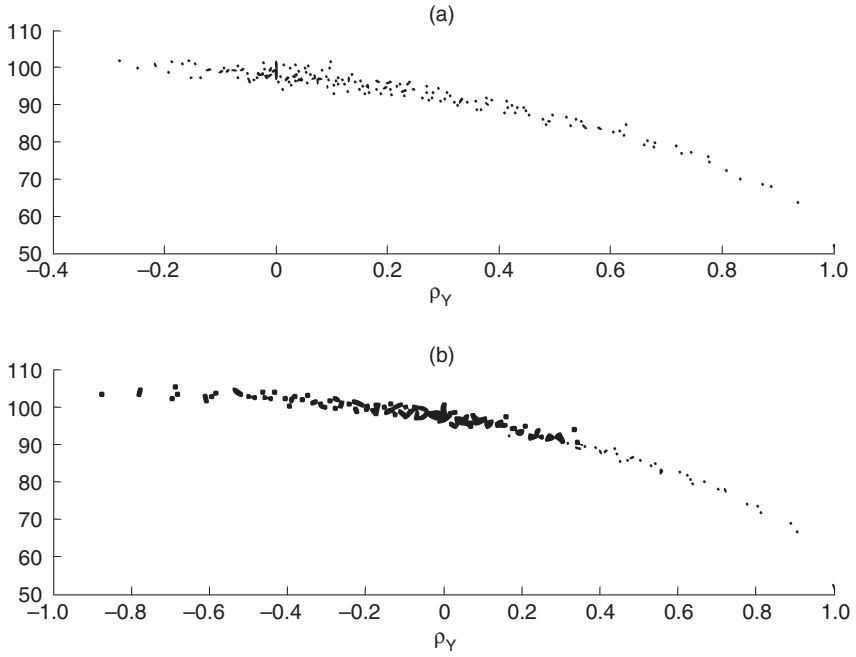

(a) Put prices under the VG model. (b) Put prices under the NIG model.

representation of the $\rho\alpha$ models allows for a straightforward simulation procedure. For the Gaussian model, we observe an average Monte Carlo standard error of 0.011 with a maximum error of 0.018. For the VG model, we observe an average Monte Carlo standard error of 0.041 with a maximum error of 0.064. Finally, for the NIG model we observe an average Monte Carlo standard error of 0.041 with a maximum error of 0.064.

Figure 7 compares bid–ask market prices with model prices when the $\rho\alpha$ models are calibrated according to the joint calibration procedure and the two-step calibration procedure yields a maximum absolute correlation error that is higher than the threshold, which we set to 0.1. Further, we set the common parameters to match two alternative correlation scenarios: maximum pairwise correlations and independence. This allows us to understand how model prices react to different correlation assumptions that are consistent with the marginal parameters. Hence, Figure 7 also shows model prices that correspond with our correlation scenarios. In Figures 7(a), 7(c) and 7(e), MBRCs are ordered depending on the time to issue, as indicated on the

horizontal axis of each graph. In general, the lower the time to issue, the higher the time to maturity of the product. In Figures 7(b), 7(d) and 7(f), MBRCs are ordered depending on the time to maturity, as indicated on the horizontal axis of each graph. Figures 7(a) and 7(b), 7(c) and 7(d), and 7(e) and 7(f) show prices under the G, VG and NIG specifications, respectively. The difference between G and VG prices ranges from 0 to 4.78 with an average of 1.48, while the difference between G and NIG prices ranges from 0 to 4.53, with an average of 1.50. Finally, the difference between VG and NIG prices ranges from -0.28 to 0.30, with an average of 0.02.

Model prices lie beneath bid market prices for just-issued products in the VG and NIG specifications. This confirms the findings of Wallmeier and Diethelm (2009), who report an overpricing that typically ranges between 3% and 6%. Overpricing disappears for short-dated products: see Figures 7(b), 7(d) and 7(f). In fact, there is a slight underpricing for products with a short time to maturity in both the VG and NIG models. The difference in terms of MBRC value between independent and highly positively correlated processes (ie, the effect of correlation) is decreasing as the time to maturity decreases for all three specifications. Hence, correlation flexibility is crucial in pricing long-term products.

Figure 8 provides a deeper insight into the two calibration approaches, focusing on the basket with Nestlé, Novartis and RocheGS as underlyings. The two-step calibration procedure provides a good smile replication (in terms of the marginals) but underestimates correlations. In fact, the two-step procedure provides an MAE equal to 26% for the VG model and 29% for the NIG one, while the joint procedure generates a 10% MAE for both models. This implies a systematic overestimation of the put component of the MBRC for just-issued products, corresponding to an underestimation of the price of the overall product. As soon as the role of correlation dies out, prices are replicated using this calibration approach.

Lévy models, in their VG and NIG specifications, provide a good, comparable fit for plain vanilla markets. However, as pointed out by Schoutens *et al* (2004), it is difficult to draw conclusions on exotic option-pricing performance, since the mispricing of exotic options may originate from the dynamic properties of the model (as well as from the calibration procedure) in terms of calibration instruments, objective function and optimization procedure.

9 CONCLUSIONS

Our aim is to investigate the model flexibility in the risk-neutral setting of a class of multivariate Lévy models. We study MBRCs for two reasons. First, they are the most liquid multivariate products. Second, Wallmeier and Diethelm (2012) already examined a subclass of such models and found them to have less flexible dependence structures. Even though the use of Lévy models (and their calibration to vanilla options

FIGURE 7 MBRC prices (full data set).

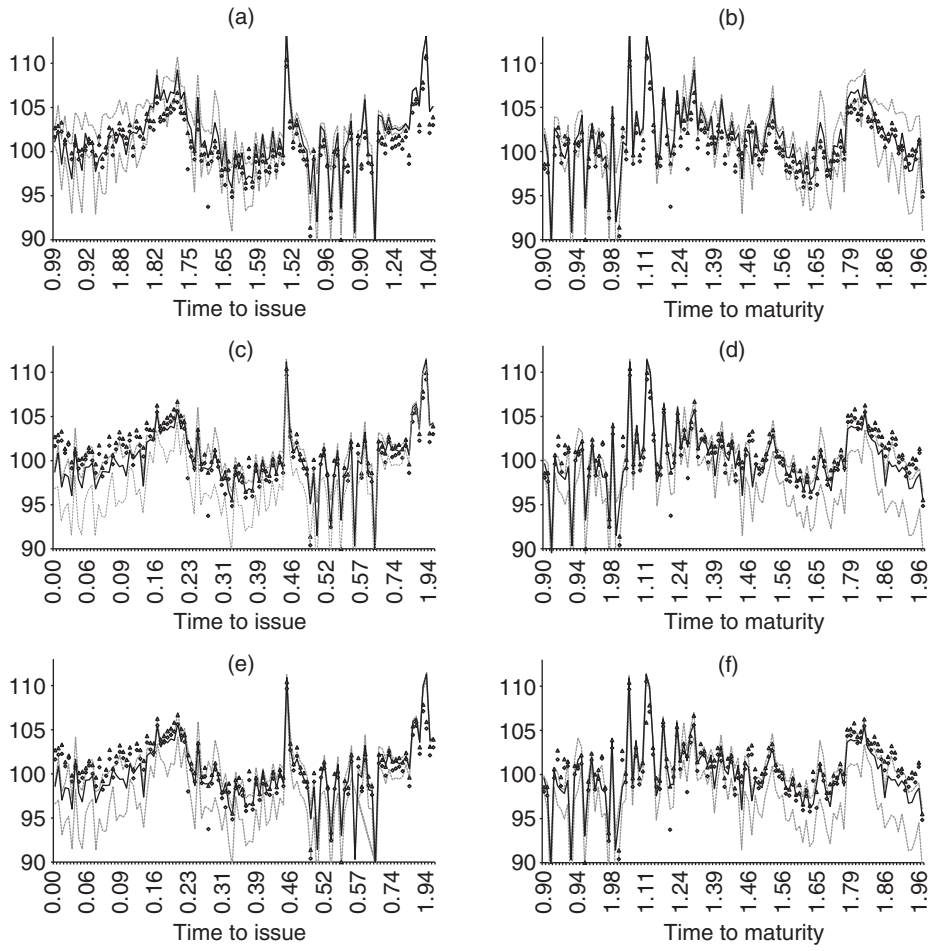

Observed bid–ask prices are represented by squares and triangles, respectively. Solid lines represent model prices, with common parameters calibrated to historical correlations. Dashed lines are model prices with common parameters set to reproduce maximum pairwise correlations (upper dashed lines) and independence between marginal processes (lower dashed lines). MBRCs are ordered depending on time to issue in parts (a), (c) and (e), as indicated on the horizontal axis of each graph. MBRCs are ordered depending on time to maturity in parts (b), (d) and (f), as indicated on the horizontal axis of each graph. Parts (a) and (b) depict MBRC prices under the G model. Parts (c) and (d) show MBRC prices under the VG model. Parts (e) and (f) show MBRC prices under the NIG model.

in this framework) does not fully account for the dynamic evolution of the implied volatility smile, it still outperforms the Gaussian model, being able to reproduce the skewness and kurtosis embedded in the distribution of the underlying at maturity, especially for short maturity products. Our aim is to explore the models' ability to

FIGURE 8 MBRC prices for the Nestlé–Novartis–RocheGS basket only.

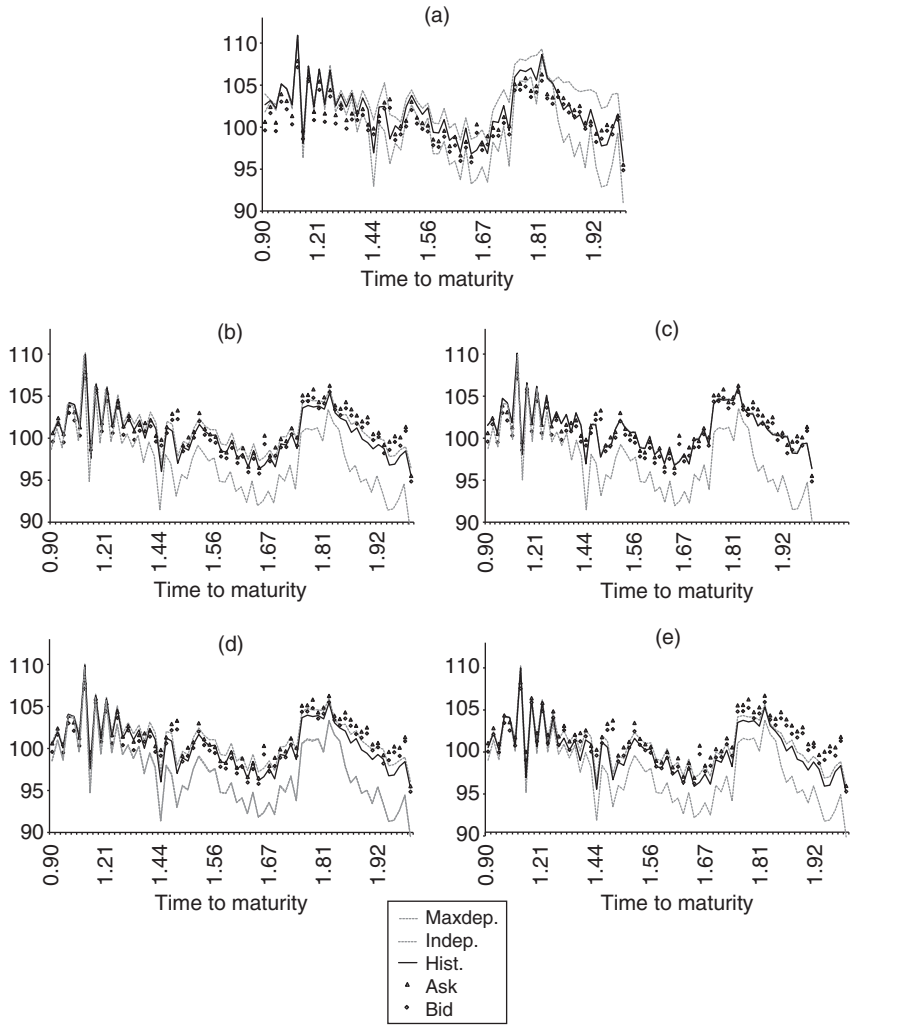

(a) MBRC prices under the G model. (b),(c) MBRC prices under the VG model with joint calibration and two-step calibration, respectively. (d),(e) MBRC prices under the NIG model with joint calibration and two-step calibration, respectively.

account for correlation (as well as the aforementioned factors) in a risk-neutral setting. The extension of this class of models to more flexible marginal specifications is on the agenda for our future research. In more detail, we explore the pricing performance of the VG and NIG specifications of the Lévy $\rho\alpha$ model introduced by Luciano

and Semeraro (2010) for multi-asset products traded in a liquid market. We extend the study of Wallmeier and Diethelm (2012), who considered the αVG model and the model introduced in Leoni and Schoutens (2008). We empirically investigate the trade-off between marginal and correlation fit by calibrating the model with two different approaches. In the former, marginal parameters are calibrated on single-asset options, and then common parameters are calibrated on the observed correlation matrix (this constitutes the two-step calibration). In the latter approach, the whole set of model parameters is calibrated at the same time for each basket of underlyings (joint calibration). The second approach allows for a better fit of the correlation structure, slightly worsening the marginal fit. The joint calibration improves the overall fit of the model and also affects the pricing performance.

We analyze critical factors affecting the price of MBRCs in terms of contract features and model parameters. Path dependency and worst-of features strongly influence MBRC prices. In particular, the price of an MBRC decreases with its time to maturity. It depends negatively on the variance and positively on the skewness of one underlying (almost independently of the others). Correlation levels are negatively related to MBRC prices. Finally, prices depend in a nonlinear way on the kurtosis of the marginal distributions.

For just-issued products, we observe a significant overpricing in both VG and NIG specifications. This stylized fact tends to decrease throughout the life of the product for all models.

This study shows that the class of $\rho\alpha$ models is well suited to pricing multi-asset derivatives. With our joint calibration approach, we are able to exploit the trade-off between marginal distributions and correlation fit, which is particularly useful if we need to enhance the goodness-of-fit of the correlation structure.

DECLARATION OF INTEREST

The authors report no conflicts of interest. The authors alone are responsible for the content and writing of the paper.

ACKNOWLEDGEMENTS

The authors thank two anonymous referees for providing valuable comments, which significantly improved this paper.

REFERENCES

Guillaume, F. (2012). The αVG model for multivariate asset pricing: calibration and extension. *Review of Derivatives Research* **16**(1), 25–52 (https://doi.org/10.1007/s11147-012-9080-2).

Hafner, R., and Wallmeier, M. (2001). The dynamics of DAX implied volatilties. *Quarterly International Journal of Finance* **1**, 1–27.

Leoni, P., and Schoutens, W. (2008). Multivariate smiling. *Wilmott Magazine*, March, 82–91.

Lindauer, T., and Seiz, R. (2008). Pricing (multi-) barrier reverse convertibles. Working Paper, University of St Gallen.

Luciano, E., and Schoutens, W. (2006). A multivariate jump-driven financial asset model. *Quantitative Finance* **6**(5), 385–402 (https://doi.org/10.1080/14697680600806275).

Luciano, E., and Semeraro, P. (2010). Multivariate time changes for Lévy asset models: characterization and calibration. *Journal of Computational and Applied Mathematics* **233**(8), 1937–1953 (https://doi.org/10.1016/j.cam.2009.08.119).

Luciano, E., Marena, M., and Semeraro, P. (2016). Dependence calibration and portfolio fit with factor-based subordinators. *Quantitative Finance* **16**(7), 1037–1052.

Madan, D. B., and Seneta, E. (1990). The variance gamma (VG) model for share market returns. *Journal of Business* **63**(4), 511–524 (https://doi.org/10.1086/296519).

Schoutens, W., Simons, E., and Tistaert, J. (2004). A perfect calibration! Now what? *Wilmott Magazine*, March, 66–78.

Semeraro, P. (2008). A multivariate variance gamma model for financial applications. *International Journal of Theoretical and Applied Finance* **11**(01), 1–18 (https://doi.org/10.1142/S0219024908004701).

Wallmeier, M., and Diethelm, M. (2009). Market pricing of exotic structured products: the case of multi-asset barrier reverse convertibles in Switzerland. *Journal of Derivatives* **17**(2), 59–72 (https://doi.org/10.3905/JOD.2009.17.2.059).

Wallmeier, M., and Diethelm, M. (2012). Multivariate downside risk: normal versus variance gamma. *Journal of Futures Markets* **32**(5), 431–458 (https://doi.org/10.2139/ssrn.1594267).